

Electrodeposition of nanostructured cobalt selenide films towards high performance counter electrodes in dye-sensitized solar cell†

Cite this: *RSC Advances*, 2013, 3, 16528

Zhongyi Zhang,^{abe} Shuping Pang,^a Hongxia Xu,^a Zhenzhong Yang,^d Xiaoying Zhang,^{ae} Zhihong Liu,^a Xiaogang Wang,^a Xinhong Zhou,^c Shanmu Dong,^a Xiao Chen,^a Lin Gu^d and Guanglei Cui^{*a}

Nanostructured cobalt selenide films with honeycomb-like morphology were successfully fabricated on FTO glass by a facile electrodeposition method at ambient temperature. Such porous structure generated by randomly intersectant freibaldite cobalt selenide nanosheets led to high concentration of active sites and better porosity accessible to the electrolyte, delivering superior electrocatalytic performance for the triiodide reduction. It was demonstrated that the nanostructured cobalt selenide films yielded comparable energy conversion efficiency to noble metal Pt electrode as the counter electrode in dye sensitized solar cells.

Received 13th December 2012,
Accepted 9th July 2013

DOI: 10.1039/c3ra42360c

www.rsc.org/advances

1. Introduction

Dye-sensitized solar cells (DSCs), as an alternative to conventional semiconductor solar cells, have attracted extensive attention in the past two decades owing to their low cost, environmental friendliness and simple fabrication procedure.^{1–4} However, further enhancements in conversion efficiency and cost effectiveness are highly desired for the large-scale application of DSCs.

Generally, as the counter electrode (CE), noble metal platinum is most commonly employed to catalyze the reduction of triiodide ions to iodide ions. However, the limited supply and the high cost strongly hinder its development. It is highly imperative to develop alternative materials. Up to now, several kinds of cost-efficient substitutes such as carbonaceous materials,^{5–7} conductive polymers^{8–10} and metallic compounds^{11–15} have been investigated as replacements for platinum. Among these materials, transition metal sulfides and selenides, owing to their unique electronic

configuration and comparatively high catalytic activity, are proposed to be promising CE materials in DSCs.^{14–19} It was recently discovered that metal selenides (Co_{0.85}Se, Ni_{0.85}Se, Cu₂ZnSnSe₄) presented superior catalytic activity than metal sulfides in terms of the triiodide reduction.^{18,19} However, up to now, the reported fabrication methods of metal selenide are relatively complicated, such as solvent-thermal method followed by a post-selenization treatment, or hydrothermal method at high temperature in an autoclave.¹⁹ With the target of simplifying the manufacturing procedure for the feasibility of large scale fabrication to reduce the overall cost, electrodeposition method was considered to be a rational approach due to its advantages of less cost, easy scale up, and relatively mild operating conditions. The electrodeposited structure also can be easily controlled by varying the precursors, electrolyte, pH value and temperature, as well as the applied potential or current density. Herein, we use an electrodeposition method to directly fabricate homogenous porous cobalt selenide (CoSe) films on FTO substrate at ambient temperature. It was demonstrated that the as-prepared cobalt selenide films, intersected with graphene-like structures, possess relatively high surface area and superior catalytic activity for the triiodide reduction. The easy fabrication and excellent catalytic activity strongly indicate their capability to serve as the CE in DSCs to replace the high cost Pt. And to the best of our knowledge, this is the first time the electrodeposited metal selenide have been reported as an efficient CE of DSCs.

^aThe Qingdao Key Lab of solar energy utilization and energy storage technology, Qingdao Institute of Bioenergy and Bioprocess Technology, Chinese Academy of Sciences, Qingdao, 266101, P. R. China. E-mail: cui@qibebt.ac.cn

^bCollege of Chemistry and Chemical Engineering, Qingdao University, Qingdao, 266071, P. R. China

^cQingdao University of Science and Technology, Qingdao, 266042, P. R. China

^dBeijing Laboratory for Electron Microscopy, Institute of Physics, Chinese Academy of Sciences, Beijing, 100190, P. R. China

^eUniversity of Chinese Academy of Sciences, 100049, P. R. China

† Electronic supplementary information (ESI) available: Electrochemical behavior of Co²⁺ and SeO₃²⁻ on FTO glass evaluated by linear-sweep voltammetry (LSV). Preparation of amorphous selenium electrode and its performance towards triiodide reduction. Growth rate curves and the verified mass loading under different pH values. See DOI: 10.1039/c3ra42360c

2. Experimental

2.1 Preparation of cobalt selenide electrodes

The cobalt selenide films were prepared by electrodeposition. The typical deposition bath was a 50 mL aqueous solution containing 20 mM Na_2SeO_3 , 20 mM $\text{Co}(\text{CH}_3\text{COO})_2$ and 100 mM LiCl . The pH value of the solution was controlled between 2 and 4 adjusted with HCl . The deposition was conducted at room temperature in a single compartment glass cell with three-electrode configuration using a CHI 660D electrochemical workstation (CH Instruments). The FTO substrate was previously cleaned with detergent and de-ionized water, followed by sonication in isopropanol for three times. A Pt wire and an Ag/AgCl electrode were used as auxiliary electrode and reference electrode, respectively. The potentiostatic electrodeposition technology was used, for which the deposition potential was maintained at -0.8 V versus Ag/AgCl electrode and the deposition time was 30 s. Finally, the FTO glass was washed with de-ionized water and dried in an air flow. The Pt-FTO electrode, as a fair comparison, was obtained by electrodepositing a thin platinum layer on the FTO substrate.

2.2 Fabrication of DSC devices

Porous TiO_2 film was prepared by loading TiO_2 slurry (Dalian HeptaChroma SolarTech Co., Ltd., China.) layer on a FTO glass by the doctor-blading technique. After calcination at 450°C for 30 min, the TiO_2 film was immersed in a 3×10^{-4} M ethanol solution of Ruthenium 535 bis-TBA (N719, Solaronix SA) for 24 h, then the dye-sensitized TiO_2 film was washed with anhydrous ethanol and dried in moisture-free air. Finally, the dye sensitized TiO_2 photoanode and the as-fabricated CE were assembled together. The liquid electrolyte, which is composed of 0.06 M LiI , 0.6 M 1-propyl-2,3-dimethylimidazolium iodide, 0.03 M I_2 , 0.5 M 4-tertbutyl pyridine and 0.1 M guanidinium thiocyanate with acetonitrile as the solvent, was then injected between the two electrodes.

2.3 Characterization

Scanning electron microscope (SEM) images and energy dispersive spectrometer (EDS) spectrum were acquired using a Hitachi S-4800 field emission electron microscope. Transmission electron microscopy (TEM) was performed using a JEOL 4000EX transmission electron microscopy (JEOL, Tokyo, Japan). XRD measurements were carried out on a Bruker D8 ADVANCE X-ray Diffractometer and the tested sample powder was prepared by directly peeling off from the cobalt selenide electrodes. The current density-voltage (J-V) characteristics of DSCs were measured under 100 mW cm^{-2} irradiation (1 sun calibrated beforehand by a standard silicon solar cell). The irradiation was from a 300 W solar simulator (Newport, USA). Cyclic voltammetry (CV) was carried out in a three electrode system in an acetonitrile solution of 0.1 M LiClO_4 , 10 mM LiI , and 1 mM I_2 at a scan rate of 50 mV s^{-1} . Platinum served as a counter electrode and the Ag/Ag^+ couple was used as a reference electrode. The electrochemical impedance spectroscopies (EIS) of the CEs were recorded using a Zennium electrochemical workstation, and were performed on dummy cells with a symmetric sandwich-like structure

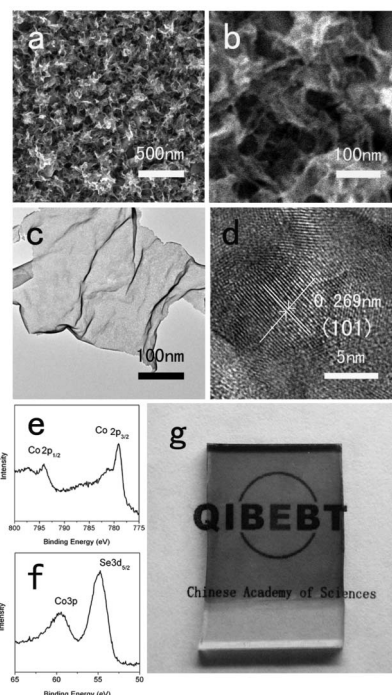


Fig. 1 (a–b) Typical SEM images of cobalt selenide electrode prepared at pH 3.5. (c) Typical TEM image of the cobalt selenide layers peeled from the electrodeposited films. (d) HTEM showing (101) lattice fringes of (c). (e–f) Typical XPS spectra of (e) Co 2p and (f) Se 3d for the prepared cobalt selenide electrodes. (g) Photograph of the cobalt selenide electrode.

between two identical electrodes, that is, CE/electrolyte/CE. The CEs used for testing in this paper are consistent with equal area (1 cm^2). The electrolyte is same as the one used for fabricating the DSCs. The frequency range was varied from 100 kHz to 10 mHz.

3. Results and discussion

3.1 Electrodeposition results

The SEM and TEM images of the electrodeposited cobalt selenide film are exhibited in Fig. 1. The as-fabricated film possesses a high uniformity as shown in the SEM image with low magnification (Fig. 1a). It can be easily seen that the cobalt selenide film is of porous honeycomb-like structure, which is formed by ~ 5 nm thick cobalt selenide sheets intersected together. The XRD patterns of the electrodeposited selenide products are shown in Fig. 2. The peaks can be well indexed to freiboldite cobalt selenide (CoSe) (JCPDS No.89-2004). The TEM image in Fig. 1c shows the thin cobalt selenide sheet is wrinkled and seems like a graphene-morphology. The lattice fringes distance (Fig. 1d) of the nanosheet is clearly observed to be 0.269 nm, which is in good coincidence with the theoretical values of (101) planes of freiboldite cobalt selenide. The XPS characterization is applied to analyze the surface chemical composition of the synthesized cobalt selenide film. In the Co 2p spectra (Fig. 1e), the electrodeposited cobalt selenide exhibits two peaks at 779.1 eV and 793.9 eV, which is

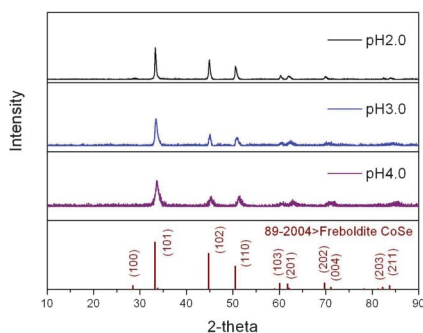


Fig. 2 XRD patterns of the cobalt selenide films prepared at various pH value.

assigned to Co 2p_{3/2} and Co 2p_{1/2} of cobalt selenide, respectively²⁰. In the Se3d spectra (Fig. 1f), the peak at 54.8 eV is consistent with Se3d_{5/2} of cobalt selenide and the peak in the range of 57.0–63.0 eV is assigned to Co3p of cobalt selenide according to the literature.^{20,21} The XPS data collaboratively corroborates the chemical state of the as-prepared cobalt selenide. It is noted that our proposed strategy can achieve a transparent film of cobalt selenide in a controlled way, which is favorable for harvesting solar light as possible.²² The cobalt selenide transparent films with high uniformity are proved as Fig. 1g and the thickness can be easily tuned by varying the electrodeposition time (Fig. S3, ESI†).

Such electrodeposition technique is versatile to prepare cobalt selenide film when varying the pH values.²³ It is also found that the cobalt selenide films deposited at different pH values show similar surface morphology (Fig. 3). It is observed that the honeycomb-like structures deposited at higher pH values (3–4) seem denser (Fig. 3), which can offer a relatively large reaction interface. Additionally, the corresponding contents of Co and Se in these films were determined by EDS spectroscopy. Table 1 lists the atomic percentage of Co, Se and Co: Se ratio in the films prepared under various pH values. It is manifested that, the ratio of Co: Se increases from 0.6 : 1 to 1.19 : 1 with a raising pH values from 2 to 4. In the case of lower pH values (2–3), the film exhibits the Se-enriched cobalt selenide according to the EDS composition. The excess Se cannot be detected by XRD (in Fig. 2) possibly due to its amorphous characteristics. The half-peak width of (101)

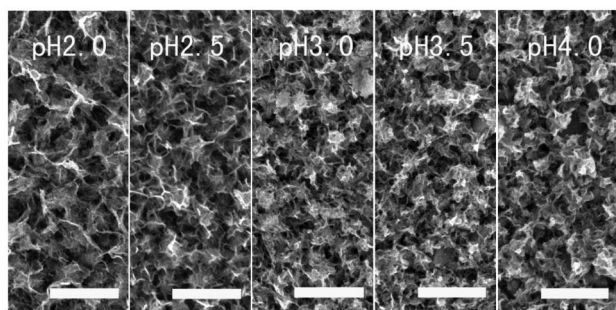


Fig. 3 SEM images of the prepared electrodes under various pH value conditions with a scale bar of 500 nm.

Table 1 Atomic percentage of Co, Se and Co : Se ratio in the cobalt selenide electrodes

The electrodeposited pH	Co	Se	Co : Se
2.0	2.07	3.45	0.6 : 1
2.5	2.02	2.96	0.68 : 1
3.0	2.19	2.81	0.78 : 1
3.5	2.43	2.45	0.99 : 1
4.0	2.81	2.37	1.19 : 1

broadens as the pH value increases (in Fig. 2), indicating the smaller particle size of cobalt selenide prepared at higher pH value, which may facilitate the catalytic reaction of I₃[−]/I[−].

3.2 Photovoltaic and catalytic performance of various CEs

Cyclic voltammetry (CV) was performed using cobalt selenide obtained at different pH values as working electrode to investigate catalytic activity for the regeneration of I₃[−]/I[−]. Pt based electrode was referenced for a fair comparison. As shown in Fig. 4, for all of the materials, two pairs of symmetrical oxidation and reduction peaks are observed. The pair of peaks at negative potential can be attributed to the redox reaction shown in eqn (1), and that pair at positive potential can be ascribed to the redox reaction shown in eqn (2).²⁴



Compared with Pt-FTO electrode, the reduction peaks of cobalt selenide electrodes prepared at pH 3.0, pH 3.5 and pH 4.0 moved towards a more positive potential. And both the heights and integration areas of these corresponding reduction peaks of eqn (1) are larger than that of Pt-FTO electrode. For a fair comparison, we also checked the electrochemical behavior of amorphous selenium electrode, which was electrodeposited in the absence of Co²⁺ (see supporting

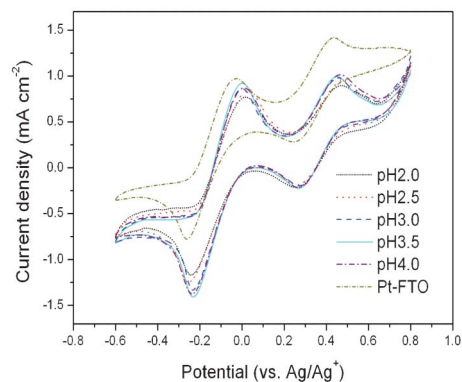


Fig. 4 Cyclic voltammetry (CV) curves of cobalt selenide electrodes prepared under various pH value and Pt-FTO electrode.

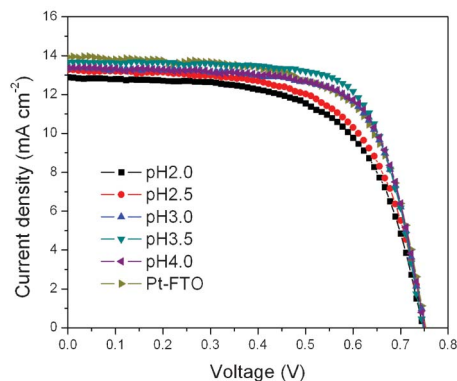


Fig. 5 Photocurrent-voltage characteristics of DSCs using various CEs.

information). The selenium based electrode does not exhibit any reduction peak, as shown in Fig. S2, ESI†. This result indicates that the amorphous selenium in the electrodeposited films is electrochemically inert to the reduction reactions of eqn (1) and eqn (2). There is great possibilities that the alleviated amorphous Se content in the cobalt selenide films is facilitate to enhance the catalytic activities and promote the performance of cobalt selenide electrode.

Fig. 5 depicts the photocurrent-voltage (J - V) curves of the DSCs with the cobalt selenide and Pt as CEs. The corresponding photovoltaic parameters are summarized in Table 2. It is obviously to note that all of the DSCs using cobalt selenide films as CEs exhibit very good performance that is already close to that of Pt CE. Evidently, the cobalt selenide prepared at high pH values shows better performance which is in accordance with the results of CV curves. To explore the variation of above mentioned cobalt selenide electrodes, the dependence of the efficiency and atomic ratio on pH values is summarized in Fig. 6. The best efficiency appears in the case of Co : Se close to 1 : 1 corresponding to the electrode prepared at pH3.5. The superior electrocatalytic activity is considered to be originated from the smaller sized crystalline structure and less content of amorphous selenium in the films. The cobalt selenide electrode (prepared at pH3.5) shows open-circuit voltage (V_{oc}) of 747 mV, short-circuit current density (J_{sc}) of 13.72 mA cm^{-2} , fill factor (FF) of 71.3% and energy conversion efficiency (η) of 7.30%. In comparison, those values (V_{oc} , J_{sc} , FF , η) for the Pt CE are 753 mV, 13.92 mA cm^{-2} , 66.0% and 6.91%, respectively. It can be deduced that cobalt selenide CEs possesses a superior photovoltaic performance comparable to Pt CE.

Table 2 Photovoltaic parameters of the DSCs cobalt selenide CEs and Pt-FTO CE

CEs	V_{oc}/mV	$J_{sc}/\text{mA cm}^{-2}$	$FF/\%$	$\eta/\%$	R_s/Ω	R_{ct}/Ω
pH2.0	747	12.92	62.1	6.00	21.18	0.90
pH2.5	752	13.31	62.6	6.27	19.72	0.97
pH3.0	750	13.42	69.5	6.99	19.59	0.93
pH3.5	747	13.72	71.3	7.30	18.19	0.84
pH4.0	750	13.44	69.9	7.04	19.41	0.70
Pt-FTO	753	13.92	66.0	6.91	19.94	1.66

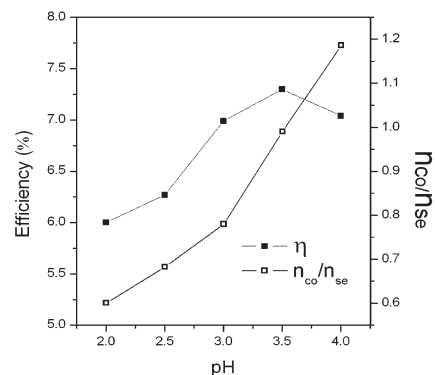


Fig. 6 The correlation between conversion efficiency, atomic ratio and pH value.

Electrochemical impedance spectroscopy (EIS) measurement were used to further investigate the charge transfer process and thereby evaluate the catalytic activities of various CEs, employing symmetrical dummy cell comprising of two identical electrodes as reported in the previous literature.⁷ Nyquist plots of various CEs measured at room temperature are shown in Fig. 7. As the investigated devices are symmetrical, a Nyquist plot is usually composed of two components. Firstly, a semicircle appear at high frequency corresponds to the charge transfer process at the electrode|electrolyte interface from which the charge transfer resistance (R_{ct}) can be derived. In addition, a Warburg impedance caused by ion diffusion through the bulk electrolyte was found in the lower frequency range. This ideal spectrum is solely observed in the case of the $\text{I}_3^-/\text{I}^-|\text{Pt}$ system.²⁵ While, in the case of cobalt selenide CEs, the Warburg impedance is almost invisible at zero bias potential. This phenomenon was also reported in other cases.²⁶ The EIS fitting data are summarized in Table 2. It is shown that, the charge transfer resistance of cobalt selenide CEs is in the range between 0.70 and $0.97 \Omega\text{cm}^2$. Compared with Pt electrode ($1.66 \Omega\text{cm}^2$), the R_{ct} of each cobalt selenide electrode is significantly alleviated, indicating a rapid triiodide reduction rate of cobalt selenide films. The optimized value of R_{ct} is $0.70 \Omega\text{cm}^2$, which is appeared in the case of pH4.0, suggesting

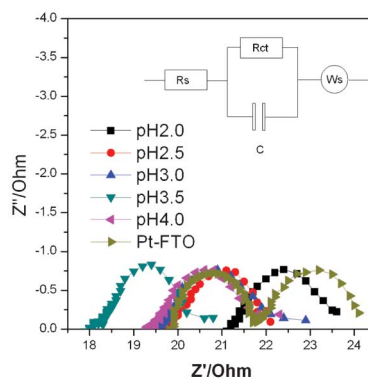


Fig. 7 Nyquist plots of the symmetric electrochemical cells assembled using cobalt selenide electrodes prepared at different pH value.

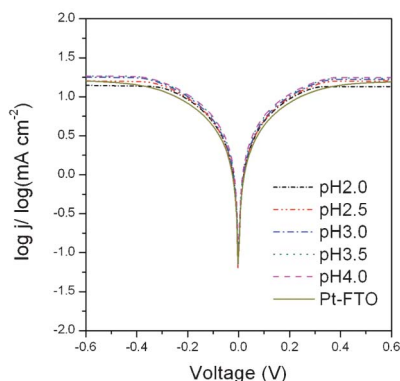


Fig. 8 Tafel curves of the symmetrical dummy cells fabricated with various electrodes.

the cobalt selenide electrode of higher pH value might facilitate the charge transfer process. The high frequency (around 100 K Hz) intercept on the real axis represents the series resistance (R_s). In the case of pH3.0, pH3.5 and pH4.0, the values of R_s is comparable to Pt-FTO, which demonstrates that the electrodeposited films are well bonded with the substrates and ensure an efficient charge transport. The smallest R_s appears in the case of pH3.5, which is corresponding to the film with the composition of Co : Se close to 1 : 1. These results indicate that the conductivity probably depends on the composition and structure of the films. The overall resistance of cobalt selenide electrodes gradually decreases with the increasing pH value, and the smallest value emerges at the pH3.5.

The enhanced exchange current density (j_0) of the cobalt selenide electrodes in comparison with the Pt-FTO electrode was also conformed in the Tafel polarization curves (Fig. 8). This indicates that the catalytic activity of cobalt selenide electrode is sufficient to catalyze the reduction of triiodide to iodide. At the same time, because the J_{lim} obtained from the Tafel polarization curves of the dummy cells highly depends on the diffusion coefficient of the triiodide/iodide redox couple in the DSC system, it is suggested that cobalt selenide electrodes synthesized with pH = 3–4 ensure higher diffusion coefficient of the triiodide/iodide redox couple than Pt-FTO electrode.

4. Conclusions

In summary, nanostructured cobalt selenide films have been electrochemically deposited on FTO glass at ambient temperature and exhibited remarkable electrochemical catalytic activities for triiodide reduction in DSCs. The cobalt selenide electrodes present lower R_{ct} and enhanced j_0 at the interface of CE/electrolyte, resulting in a comparable performance to conventional Pt-FTO CE. The simple preparation procedure, low fabrication cost and excellent catalytic properties endow the electrodeposited cobalt selenide with an ideal alternative of the CE for the future DSCs. In addition, the sample electrochemical method introduced in this manuscript is

expected suitable for preparing other metal selenides as counter electrode to replace expensive Pt in DSCs.

Acknowledgements

This work was supported by National Program on Key Basic Research Project of China (973 Program) (No. MOST2011CB935700), the “100 talents” program of Chinese Academy of Sciences, the National Natural Science Foundation (Grant No.20901044, 20902052 and 51202266), the Natural Science Foundation of Shandong Province (Grant No. ZR2011BQ024).

References

- 1 B. O'Regan and M. Grätzel, *Nature*, 1991, **353**, 737.
- 2 A. Hagfeldt, G. Boschloo, L. C. Sun, L. Kloo and H. Pettersson, *Chem. Rev.*, 2010, **110**, 6595.
- 3 Q. J. Yu, Y. H. Wang, Z. H. Yi, N. N. Zu, J. Zhang, M. Zhang and P. Wang, *ACS Nano*, 2010, **4**, 6032.
- 4 Y. Zhao, J. Zhai, J. L. He, X. Chen, L. Chen, L. B. Zhang, Y. X. Tian, L. Jiang and D. B. Zhu, *Chem. Mater.*, 2008, **20**, 6022.
- 5 J. D. Roy-Mayhew, D. J. Bozym, C. Punckt and I. A. Aksay, *ACS Nano*, 2010, **4**, 6203.
- 6 J. E. Trancik, S. C. Barton and J. Hone, *Nano Lett.*, 2008, **8**, 982.
- 7 M. X. Wu, X. Lin, T. H. Wang, J. S. Qiu and T. L. Ma, *Energy Environ. Sci.*, 2011, **4**, 2308.
- 8 L. Bay, K. West, B. Winther-Jensen and T. Jacobsen, *Sol. Energy Mater. Sol. Cells*, 2006, **90**, 341.
- 9 Y. Saito, T. Kitamura, Y. Wada and S. Yanagida, *Chem. Lett.*, 2002, **10**, 1060.
- 10 H. X. Xu, X. Y. Zhang, C. J. Zhang, Z. H. Liu, X. H. Zhou, S. P. Pang, X. Chen, S. M. Dong, Z. Y. Zhang, L. X. Zhang, P. X. Han, X. G. Wang and G. L. Cui, *ACS Appl. Mater. Interfaces*, 2012, **4**, 1087.
- 11 M. X. Wu, X. A. Lin, A. Hagfeldt and T. L. Ma, *Angew. Chem., Int. Ed.*, 2011, **50**, 3520.
- 12 X. Y. Zhang, X. Chen, S. M. Dong, Z. H. Liu, X. H. Zhou, J. H. Yao, S. P. Pang, H. X. Xu, Z. Y. Zhang, L. F. Li and G. L. Cui, *J. Mater. Chem.*, 2012, **22**, 6067.
- 13 G. R. Li, J. Song, G. L. Pan and X. P. Gao, *Energy Environ. Sci.*, 2011, **4**, 1680.
- 14 Z. Y. Zhang, X. Y. Zhang, H. X. Xu, Z. H. Liu, S. P. Pang, X. H. Zhou, S. M. Dong, X. Chen and G. L. Cui, *ACS Appl. Mater. Interfaces*, 2012, **4**, 6242.
- 15 M. K. Wang, A. M. Anghel, B. Marsan, N. L. C. Ha, N. Pootrakulchote, S. M. Zakeeruddin and M. Grätzel, *J. Am. Chem. Soc.*, 2009, **131**, 15976.
- 16 H. C. Sun, D. Qin, S. Q. Huang, X. Z. Guo, D. M. Li, Y. H. Luo and Q. B. Meng, *Energy Environ. Sci.*, 2011, **4**, 2630.
- 17 X. K. Xin, M. He, W. Han, J. H. Jung and Z. Q. Lin, *Angew. Chem., Int. Ed.*, 2011, **50**, 11739.
- 18 F. Gong, H. Wang, X. Xu, G. Zhou and Z. S. Wang, *J. Am. Chem. Soc.*, 2012, **134**, 10953.
- 19 Y. F. Du, J. Q. Fan, W. H. Zhou, Z. J. Zhou, J. Jiao and S. X. Wu, *ACS Appl. Mater. Interfaces*, 2012, **4**, 1796.

- 20 A. B. Mandale, S. Badrinarayanan, S. K. Date and A. P. B. Sinha, *J. Electron Spectrosc. Relat. Phenom.*, 1984, **33**, 61.
- 21 C. A. Strydom and H. J. Strydom, *Inorg. Chim. Acta*, 1989, **159**, 191.
- 22 H. Tantang, A. K. K. Kyaw, Y. Zhao, M. B. Chan-Park, A. I. Y. Tok, Z. Hu, L. J. Li, X. W. Sun and Q. C. Zhang, *Chem.–Asian J.*, 2012, **7**, 541.
- 23 F. Y. Liu, B. Wang, Y. Q. Lai, J. Li, Z. A. Zhang and Y. X. Liu, *J. Electrochem. Soc.*, 2010, **157**, D523.
- 24 G. Boschloo and A. Hagfeldt, *Acc. Chem. Res.*, 2009, **42**, 1819.
- 25 X. O. Yin, Z. S. Xue and B. Liu, *J. Power Sources*, 2011, **196**, 2422.
- 26 J. Burschka, V. Brault, S. Ahmad, L. Breau, M. K. Nazeeruddin, B. Marsan, S. M. Zakeeruddin and M. Grätzel, *Energy Environ. Sci.*, 2012, **5**, 6089.